Received: 9 September 2024 | Revised: 10 December 2024 | Accepted: 26 December 2024 | Published online: 31 December 2024

RESEARCH ARTICLE

Journal of Optics and Photonics Research
2025, Vol. 00(00) 1–12
DOI: 10.47852/bonviewJOPR42024305

BON VIEW PUBLISHING

Design of a Novel 31.5 THz Bandwidth Hybrid TDFA-HDFA at 2000 nm and Its Applications in Unregenerated DWDM Lightwave Transmission Systems

Robert E. Tench[1,*]

[1]*Research Department, RET and Associates LLC, USA*

Abstract: We report the design and applications of a novel multi-Watt (>1 Watt output power) 2000 nm band hybrid Thulium- and Holmium-doped fiber amplifier with record wideband 380 nm (31.5 THz) continuously operating bandwidth from 1720 to 2100 nm. We outline the theory, physics, and simulations behind this design and show by comparison with previously published experimental results that the design presented is accurate to within ±0.5 dB in saturated output power and ±1.0 dB in small signal gain. Applications in future ~300–400 nm bandwidth wideband 2000 nm Pb/s DWDM lightwave fiber optical transmission systems spanning 10,000 km using new hollow-core fiber designs are discussed. In particular, we demonstrate robust beginning-of-life optical signal-to-noise ratio and Q-factor margins for designs of 0.161 Pb/s DWDM unregenerated (without optical-to-electrical-to-optical or O-E-O electronic functions) all-optical transmission in the 2000 nm band over 10,000 km for representative terrestrial and submarine lightwave applications. We achieve a total capacity × distance product of 1608 Pb/s. km (1.61 Exabits/s. km) over a single one-core optical fiber for the 10,000 km system designs. Applications to designs of 40,000 km deployable unregenerated all-optical DWDM 0.124 Pb/s subsea lightwave transmission systems with 5.21 Exabit/s. km capacity × distance product are outlined.

Keywords: Tm-doped fiber amplifier, Ho-doped fiber amplifier, hybrid Tm-Ho-doped fiber amplifier, DWDM lightwave system design, 2000 nm

1. Introduction

Two-micron Holmium-doped (HDF) [1–6] and Thulium-doped (TDF) [7–15] fiber amplifiers and lasers have important roles to play in many space and physics applications. These include, but are not limited to: free-space transmission in low atmospheric attenuation wavelength bands, measurement of concentrations of gases such as CO_2 and CH_4 in the atmosphere, generation of high energy 3–5 μm signals, high power Tm-doped fiber amplifiers and lasers for directed energy weapons, remote molecule sensing and LIDAR imaging, future gravity wave interferometers, and quantum computing experiments with 133Ba+ ions at 1762 nm. In these applications, the Ho-doped fiber amplifiers have an operating bandwidth of ~100 nm [1–6], and the Tm-doped fiber amplifiers have an operating bandwidth of ~200 nm [7–15].

One application that is now emerging, but has not previously been considered widely, is the use of extremely wide bandwidth (≥350 nm operating spectral width) Tm- and Ho-doped fiber amplifiers in future installed 2000 nm DWDM optical fiber transmission systems. All but one of the essential components for building these 2000 nm DWDM lightwave systems [16] have now been developed. They are single-frequency laser sources, the physics and engineering of integrated transponders, integrated amplitude and phase modulators, high-speed photodetectors, wideband fiber amplifiers with record operating bandwidth [1–15], and DSPs for the coherent transponders. The remaining essential component, extremely low-loss wideband transmission bandwidth optical fiber in the 2000 nm band, has not yet been manufactured. However, the path to creating this novel hollow-core fiber at losses approaching ≤0.04 dB/km in the 2000 nm band and specifically optimized for this precise wavelength region is now possible [17, 18]. Wideband DWDM fiber optical transmission systems in the 2000 nm band using extremely broadband Ho- and Tm-doped fiber amplifiers and novel hollow-core fibers will significantly advance the state of lightwave transmission systems and networks and are expected to usher in a new era in ultra-high capacity and ultra-long transmission distance operation of future fiber communications systems.

In this paper, we present the design of a novel multi-Watt-level (>1 Watt output power) hybrid Tm- and Ho-doped fiber amplifier with 380 nm operating bandwidth (from 1720 to 2100 nm, a record 31.5 THz) and low noise figure that is suitable for wideband amplification of multiple sources in the 2000 nm band. We then give a detailed analysis of the total achievable transmission capacity (in Pb/s) without the need for O-E-O regeneration (10,000 km and 40,000 km) for representative all-optical novel DWDM lightwave systems operating over a ≥350 nm bandwidth in the 2000 nm band, followed by comments on the remaining practical considerations necessary to put such systems into full deployment in the field.

*Corresponding author: Robert E. Tench, Research Department, RET and Associates LLC, USA. Email: robert.tench@retandassociatesllc.com

Our paper is organized as follows. First, we outline the design and performance of a multi-Watt 380 nm (31.5 THz) bandwidth novel hybrid TDFA-HDFA. We start with the novel optical architecture and then present the output performance (gain, output power, output spectra, and noise figure) as a function of signal wavelength. We then discuss the physics that makes this novel extremely wideband fiber amplifier possible. Next, we discuss the possible performance of the operation of the amplifier with carefully selected gain-flattening filters and show a simpler alternative design that does not require the use of optical circulators. Subsequent analysis covers first an outline for the development of new hollow-core fibers with ≤0.05 dB/km losses over a 400 nm operating bandwidth in the 2000 nm spectral region, followed by a detailed Pb/s capacity unregenerated all-optical lightwave system design example for 10,000 and 40,000 km total transmission lengths using the novel extremely wideband 2000 nm fiber amplifiers and the hollow-core fibers. We then present a discussion and end with summary remarks.

2. Design and Performance of the 31.5 THz BW (380 nm) Hybrid TDFA-HDFA

2.1. Optical architecture of the design with 1567 nm/1860 nm pumping

Figure 1 is an optical schematic of the novel 380 nm BW hybrid TDFA-HDFA with a record 31.5 THz bandwidth. The previous bandwidth record for fiber amplifiers in the 2000 nm band is ~19 THz or ~230 nm for a wideband TDFA [19]. In the 1350 nm band, the record is 23.0 THz or 150 nm in a Bi-doped fiber amplifier operating from 1325 to 1475 nm [20]. In this design, the Tm-doped active fiber F1 in the first stage is Exail IXF-TDF-5-125 with a length of 1.4 meters. The first stage is co-pumped at 1567 nm with 10 W of pump power from a fiber laser source or a MOPA. The Ho-doped active fiber F2 in the second stage is Exail IXF-HDF-8-125 with a length of 2.0 meters. The second stage is counter pumped at 1860 nm [21] with 6.25 W of pump power from a fiber laser source or a MOPA. Counter-pumping and an 1860 nm pump wavelength are chosen to maximize the output power from the second stage [21]. The isolator losses (I1) for the signal in this design are 1.2 dB and the WDM losses (WDM1) are 0.6 dB for both the pump and the signal. The signal and pump losses in each stage of the circulators (CIR 1 and 2) in the Ho-doped second stage are 1.0 dB. For CIR1 and CIR2, port 1 is signal input, port 2 is signal output, and port 3 is for the 1860 nm pump.

We assume that the isolator, WDM, and circulators all operate successfully over the entire signal bandwidth of the wideband amplifier. This assumption will be addressed in detail later in the discussion section.

We note that the design of our novel hybrid 380 nm bandwidth fiber amplifier is unique in the aspect that it has a first stage with Tm-doped fiber followed by a second stage with Ho-doped fiber. This is the opposite of all single-clad hybrid designs for 2000 nm published so far [7, 19, 21]. The novel choice of a first-stage TDF followed by a second-stage HDF provides a new record-setting, extremely wide continuous operating bandwidth as presented in detail in the next section.

Figure 1
Optical architecture of the novel 380 nm bandwidth hybrid HDFA-TDFA

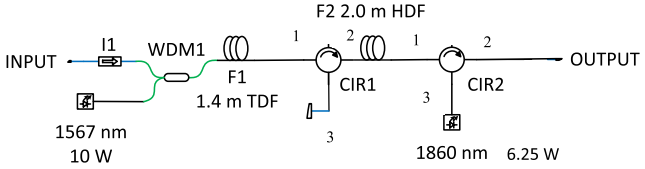

2.2. Signal output power and noise figure as a function of signal wavelength

The simulated output power and noise figure for the hybrid amplifier in Figure 1 are plotted in Figure 2 for a monochromatic input signal from 1700 to 2125 nm in wavelength and an optical power of 0 dBm. Details of the proprietary simulation software programs, called Ho-FIB1 and Tm-FIB1, are presented in Tench et al. [21] and Romano et al. [19] and are outlined in Section 5. Figure 2 shows that the fiber-coupled output powers range from 1.4 W to 3.3 W over the majority of the spectral operating band and that the 6 dB width of the output power curve is a record 380 nm (1720 nm–2100 nm, 31.5 THz). The device noise figure over this operating band is typically 6 dB or less, indicating good performance of the hybrid fiber amplifier design.

2.3. Output spectra as a function of signal wavelength

We next plot the output spectra for the amplifier for signal wavelengths of 1750, 1900, and 2050 nm. These spectra are shown in Figure 3(a), (b), and (c) with a resolution BW of 1.0 nm. We observe that with an input monochromatic signal power of 0 dBm, the optical signal-to-noise ratio (OSNR) values of the output spectra are 48, 53, and 58 dB/0.1 nm, respectively, for the three signal wavelengths studied. These are good OSNR values for both monochromatic signal amplification and for DWDM operation with a multiwavelength input frequency comb.

2.4. Outline of the physics contributing to the wideband amplifier operation

To better understand the physics behind the novel 380 nm (31.5 THz) fiber amplifier with record bandwidth, we begin by plotting the

Figure 2
The simulated output power and noise figure for the hybrid TDFA-HDFA from 1700 to 2125 nm. The output power and the noise figure are for the complete device (input fiber pigtail-to-output fiber pigtail performance). Since the input power is 0 dBm, the output power in dBm and the amplifier gain in dB are numerically equal. The 6 dB output power bandwidth of this novel design is 380 nm (1720–2100 nm) or a record 31.5 THz

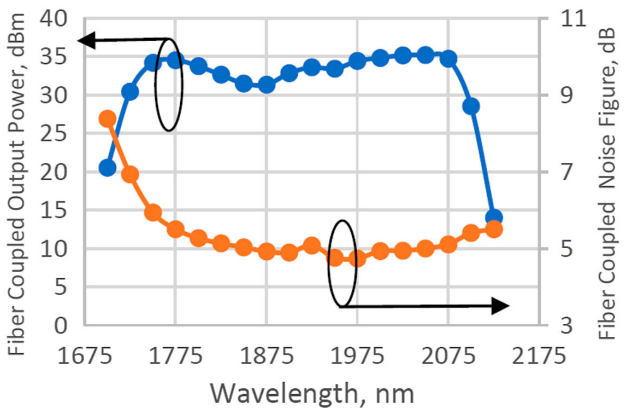

Figure 3
(a) Output spectrum for 1750 nm input at 0 dBm. RBW = 1.0 nm, (b) output spectrum for 1900 nm input at 0 dBm. RBW = 1.0 nm, and (c) output spectrum for 2050 nm input at 0 dBm. RBW = 1.0 nm

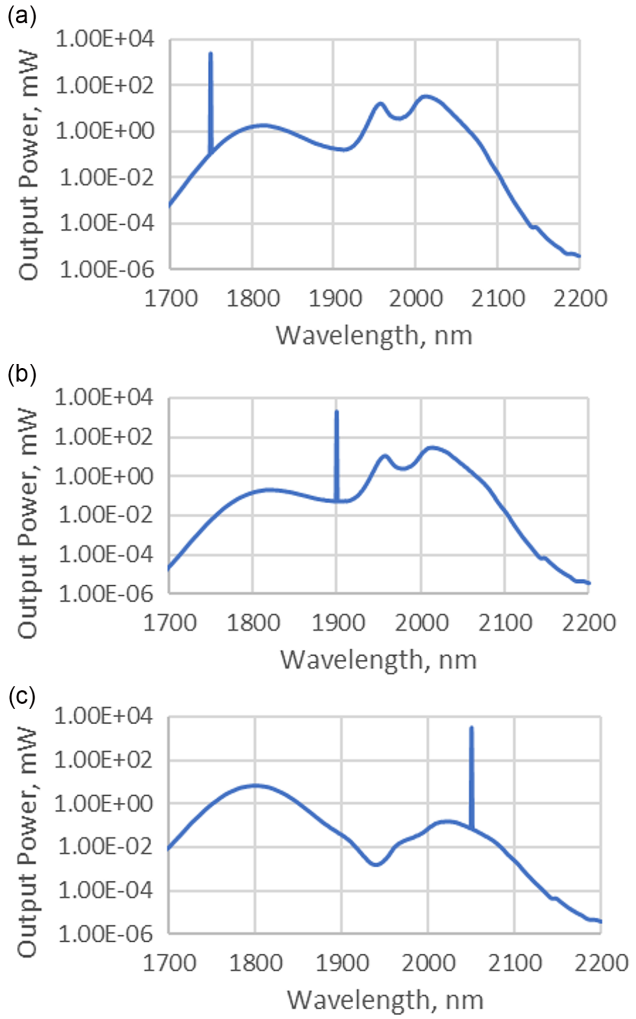

output power for the first TDFA stage that is input to the second stage and also the consequent output power for the second HDFA stage in Figure 4.

Here the output power from the first TDFA stage (with 1 mW input power) is quite high from 1725 to 1950 nm [7, 19, 21]. In this spectral range, the second-stage HDFA does not amplify but acts instead as an attenuator. Nevertheless, the high-output power from the first stage is large enough to overcome the significant attenuation of the second stage in the lower spectral region, resulting in multiwatt output from the fiber amplifier overall.

In the higher spectral range of 1975–2100 nm, Figure 4 shows that the output power from the first stage diminishes significantly as the wavelength increases as expected [7, 19, 21]. Nevertheless, the remaining output power over this range is quite high enough to serve as an excellent input power for the high gain second stage, resulting in continued multiwatt output power from the amplifier as in the previous lower spectral range.

The operation of the novel 380 nm (31.5 THz) bandwidth hybrid amplifier is further illustrated by considering the gain (attenuation) vs. wavelength of the Ho-doped fiber in the second stage.

Figure 4
Output powers from the first TDFA stage (blue) and second HDFA stage (orange) as a function of signal wavelength from 1700 nm to 2125 nm

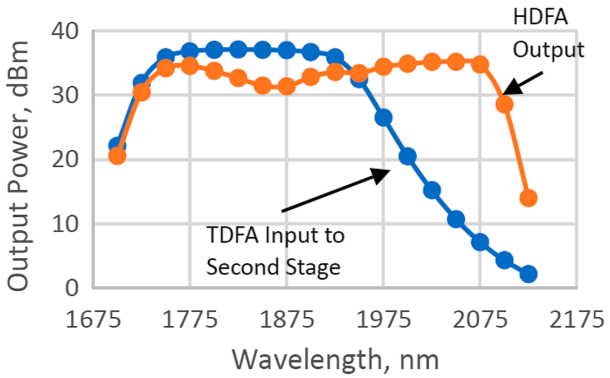

Figure 5
Gain (attenuation) of the second HDFA stage as a function of signal wavelength for 0 dBm signal input power. The 0 dB gain or transparency line is shown in red

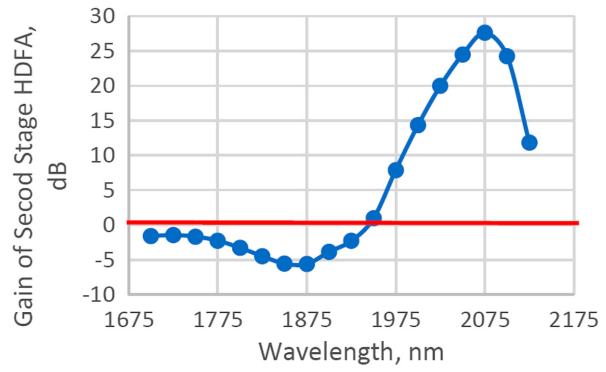

This gain (attenuation) vs. wavelength is plotted in Figure 5 which clearly demonstrates how the Ho-doped second stage acts as an attenuator for 1700–1950 nm and then as an excellent fiber amplifier from 1975 to 2125 nm.

2.5. Comments on the anticipated performance of the hybrid TDFA-HDFA with gain-flattening filters

In most applications, it is desirable to flatten the wavelength response of a fiber amplifier over its full operating range. Many previous demonstrations of this technique are fully developed for C- and L-band Er-doped fiber amplifiers operating in 1550 nm DWDM lightwave transmission systems and networks [22]. The gain-flattening optical filters, both fiber-based and fiber-coupled bulk-optics-based deployed today for 1550 nm can readily be adapted to the 2000 nm band and used in future lightwave systems employing the novel 380 nm BW hybrid TDFA-HDFA. The issue of developing gain-flattening filters over a ~400 nm bandwidth is addressed in detail in the discussion section.

We now illustrate the potential for a gain flattened 380 nm BW hybrid TDFA/HDFA by simulating the performance of the amplifier

in Figure 1 with a monochromatic input signal using the following two gain-flattening filters as shown in Figure 6. The filter in Figure 6(a) is inserted after the first Tm-doped stage and before the second Ho-doped stage. The filter in Figure 6(b) is inserted after the second Ho-doped stage.

With these gain-flattening filters inserted into the fiber amplifier design, we achieve the following output power vs. signal wavelength performance shown in Figure 7.

We see that gain flatness of ≤0.5 dB p-p is readily achieved with this initial design for a monochromatic input signal. The more complex gain flattening required for a DWDM input signal may then be accomplished using standard techniques [22].

2.6. Optical architecture of the hybrid design with 1190 nm pumping

Many current Tm-doped and Ho-doped fiber amplifiers are in-band pumped at 1567 nm for Tm and 1860–1940 nm for Ho [7, 19, 21]. In-band pumping has a lower quantum defect than out-of-band pumping but experiences the difficulty of pump wavelengths that are quite close to the signal wavelengths with consequent high demands on the performance of the wavelength division multiplexers. An alternative arrangement is to use 1150–1190 nm pumps for both Tm-doped [23] and Ho-doped [24] fiber amplifiers and lasers. This out-of-band pumping technique yields improved noise figures (up to 2 dB improvement) and relaxes the demands on the performance of the WDMs.

An example of the hybrid amplifier design using 1190 nm pumping for both stages is given in Figure 8. Here the WDMs are fused fiber couplers. In this architecture, no optical circulators are required to couple in and then separate the pump light used in the HDFA second stage, simplifying the overall design and reducing the cost of the manufactured amplifier.

In this alternative design, isolators I2 and I3 perform the same functions as CIR 1 and CIR 2 in the design of Figure 1 by isolating the first and second stages and minimizing the effects of outside feedback. WDM 2 and WDM 3 in Figure 8 remove residual pump light at 1190 nm from both stages to ensure that isolator I2 is not affected by a high power out-of-band signal.

We note that compact semiconductor laser and multiwatt fiber laser pump sources at 1150–1190 nm are now commercially available and deployed in the field.

Initial simulations indicate that with a total combined pump power of 5.5 W at 1190 nm for the two stages in Figure 8, the noise figure will be approximately 4 dB and the fiber-coupled output signal power in the 1720–2100 nm band will be about 1.0 W (+30 dBm). More detailed simulations for the 1190 nm pumped hybrid amplifier will be presented in a future publication.

Figure 6
(a) Spectral characteristics of interstage gain-flattening filter inserted after the first Tm-doped stage and (b) output gain-flattening filter inserted after the second Ho-doped stage

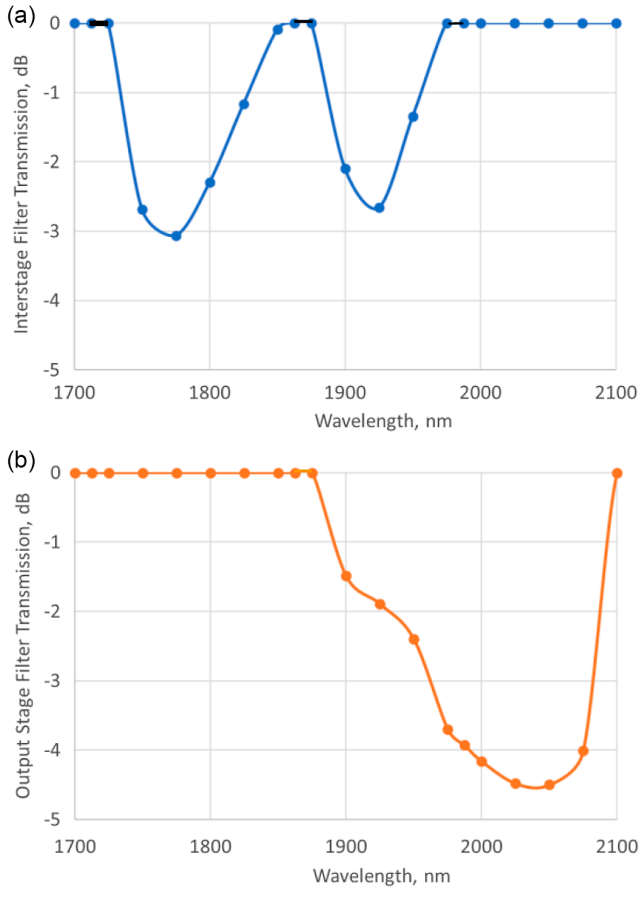

Figure 7
(a) Output power vs. signal wavelength performance for the gain flattened 380 nm BW amplifier using the two filters in Figure 6 and (b) output power vs. signal wavelength performance on an expanded vertical scale

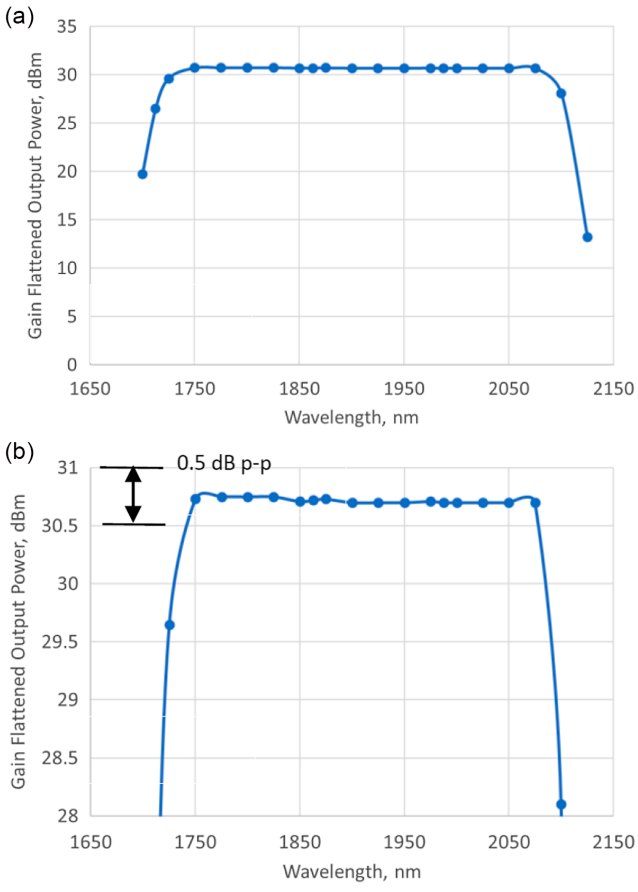

Figure 8
An alternative broadband TDFA-HDFA optical architecture using 1190 nm pumping

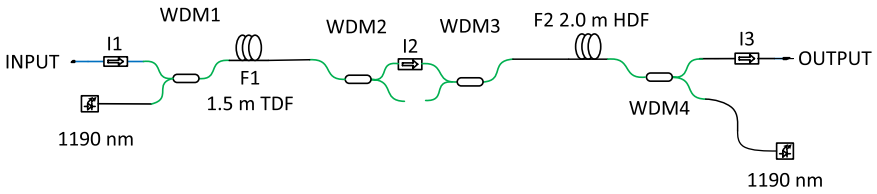

In the next section, we now discuss the practical applications of the novel 31.5 THz BW 2000 nm band fiber amplifier in practical and deployable DWDM lightwave systems.

3. Applications in Future 2000 nm DWDM Fiber Lightwave Systems Using New Hollow-Core Fiber Designs

3.1. Outline and matrix for future hollow-core transmission fibers with 1750–2150 nm operating BW

We begin our quantitative system analysis section by surveying the current state of key components and devices for present 1550 nm and future 2000 nm high bandwidth DWDM fiber optical transmission systems. This survey [16] is shown below in Table 1.

We see from Table 1 that all key components and devices are realized for 1550 nm DWDM transmission systems as expected. For 2000 nm systems, the outstanding item is the development required to design and manufacture a hollow-core transmission fiber with ~400 nm operating BW and loss of ≤0.03 dB/km. We outline an approach to this necessary design and development in the paragraphs below.

Hollow-core fibers have been extensively researched, studied, and built for the past 15 years. A comprehensive survey of the state of the art in this important field for mid-2024 is contained in the extensive and thorough analysis found in Chen et al. [17], Fokoua et al. [18], as well as Poggiolini and Poletti [25]. In this survey and analysis, we find the following plot in Chen et al. [17], shown as Figure 9, of present and anticipated losses vs. wavelength for DNANF hollow-core fiber designs optimized for transmission at 1550 nm.

Here the authors show designs for potential future DNANF hollow-core fibers optimized for 1550 nm operation and that begin to move toward the operating band required for future 2000 nm DWDM lightwave systems with extremely broadband TDFA-HDFA fiber amplifiers. We note that the ideal minimum loss at 2000 nm for this fiber is 0.04 dB/km (dashed red line). We take this value as a beginning indicator for the future losses that can be achieved in manufactured and deployed fibers in a 2000 nm system with new hollow-core fiber designs that are

Table 1
Survey of current state of components and devices for DWDM lightwave transmission systems at 1550 nm and 2000 nm

Key component/Device	Realized at 1550 nm	Realized at 2000 nm [16]
Single-frequency Laser Source	YES-70 nm Bandwidth Range	YES->350 nm Bandwidth Range
Integrated Transponder	YES	Physics-YES; Minor Engineering-Required
Amplitude/Phase Modulator	YES	YES
High-speed Photodetector	YES	YES
Wideband Fiber Amplifiers	YES-70 nm BW	YES- >350 nm BW [This Work]
Wideband Transmission Fiber	YES->80 nm BW	DEVELOPMENT REQUIRED: POTENTIAL FOR >400 nm BW
DSP for Coherent Transponder	YES	YES

Figure 9
This case illustrates scenarios for new DNANF (double nested antiresonant nodeless fiber) hollow-core fiber designs optimized for 1550 nm. Total predicted loss for an ideal fiber is in the dashed red curve, and experimental measurements for a newly manufactured fiber are in blue. For comparison, the loss of standard pure silica SMF is also shown (dashed black curve)

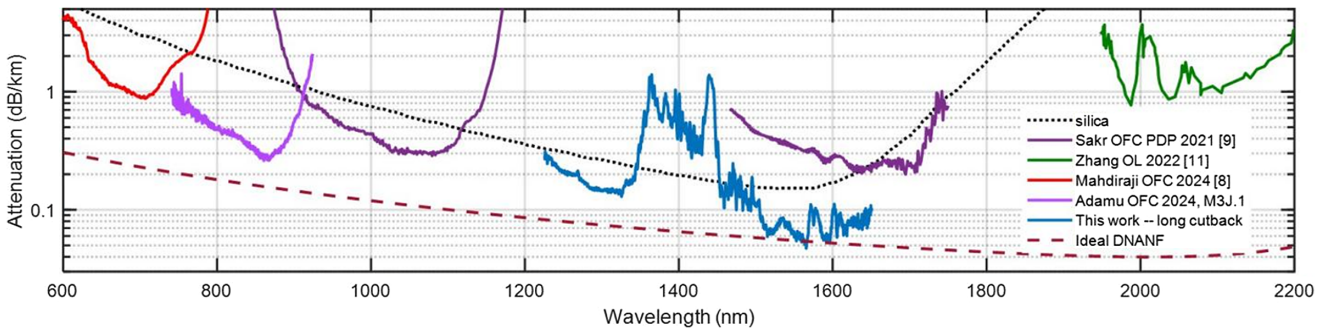

Table 2
Fiber amplifier parameters for the hybrid TDFA-HDFA in a future 2000 nm DWDM system

Fiber amplifier parameters for hybrid TDFA-HDFA	Numerical value
Effective Operating Bandwidth	350 nm (1750–2100 nm, 28.55 THz)
Total Fiber-coupled Output Power (TOP) for each fiber amplifier in cable with one pair of fibers	2.2 W (+33.4 dBm) terrestrial 1.00 W(+30.0 dBm) subsea
Device Noise Figure over Operating Bandwidth	≤6.0 dB terrestrial 4.0 dB subsea
Average OSNR over Operating Bandwidth	50 dB/0.1 nm for a monochromatic input at 0 dBm
Achievable Gain Flatness with Interstage Gain-flattening Filters, over Full Operating Range	≤0.50 dB [this work]
Gain vs. Input Power Behavior	See Figure 10

Table 3
Lightwave system parameters for the hybrid DWDM 2000 nm transmission system design

System parameters for 2000 nm DWDM transmission	Numerical value
Effective Loss of the Hollow-core Fiber	0.05 dB/km
Effective Operating Bandwidth of the Hollow-core Fiber	1750–2100 nm (28.55 THz) as shown in Figure 9
Range of Span Lengths Considered in the Designs	100 km–200 km
Range of Span Losses	5.0 dB–10.0 dB
Effect of Optical Nonlinearities in the Hollow-core Transmission Fiber (SBS, SRS, FWM, SPM-Kerr effect, etc.,)	No measurable nonlinear effects up to +35 dBm/channel [26, 27]
Dispersion of the Hollow-core Fiber over the Effective Operating Bandwidth [26–30]	2.0 pS/nm.km (estimated)
Number of Fiber Amplifier Repeaters in the System Design	NAMP
Spacing of Dynamic Gain-flattening Filters in the System	Every 6–8 Repeaters
Number of Spans in the System	NSPAN = NAMP
Number of DWDM Channels (Carriers)	NCHAN = 571
Channel Spacing	50 GHz [31]
Native Baud Rate of Each Channel	32 Gbaud [31]
Transmission Capacity of Each Channel (Carrier)	281.6 Gbps/carrier
Coherent Modulation Approach	PCS-64QAM [31]
Q-Factor for 1E-03 BER at the Receiver Using FEC (25% overhead)	4.7dB [31]
Total System Capacity	0.161 Pb/s
Total System Length Range	10,000 km–40,000 km

specifically optimized for the 2000 nm operating spectral band. We also note that experimentally measured losses of 0.08 dB/km at 1550 nm were recently reported in the literature for DNANF hollow-core fibers [17], and rapid future improvements in loss values for similar hollow-core fiber designs are expected to be published soon. We now use the initial loss value of 0.04 dB/km at 2000 nm as a benchmark for the analysis of future 2000 nm DWDM lightwave transmission systems presented in the next section.

3.2. Optical architecture of future ~400 nm BW fiber amplified 2000 nm fiber transmission system and quantitative calculations of novel 2000 nm system performance

To establish a clear picture of what could potentially be achieved in future 2000 nm DWDM transmission systems, we first outline in Table 2 the fiber amplifier and transmission system operating parameters employed in our analysis.

An important amplifier parameter for system design is the gain vs. optical input power performance of the fiber amplifier repeaters. We now use the simulated gain vs. optical input power for the fiber amplifier of Figure 1 that is shown in Figure 10 below.

Next, Table 3 outlines the system parameters for the future 2000 nm DWDM lightwave system, including the performance of the new hollow-core fiber design shown in Figure 10.

We use an effective loss of 0.05 dB/km for the hollow-core transmission fiber in the 1750–2100 nm band to account for

Figure 10
Device fiber-fiber gain as a function of input signal power at 1925 nm for the wideband hybrid TDFA-HDFA of Figure 1

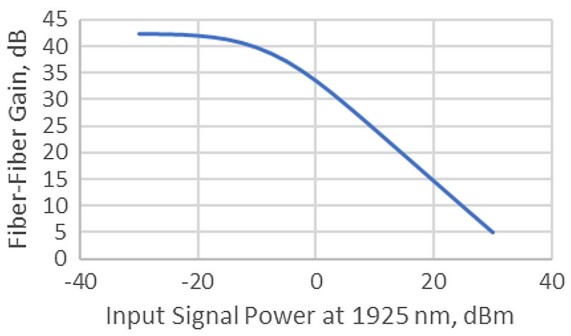

Figure 11
(a) Overall optical architecture for the future 2000 nm DWDM lightwave transmission system under study and (b) OSNR evolution in the 2000 nm DWDM lightwave system for a cascade of N identical amplified sections with amplifier gain = span loss

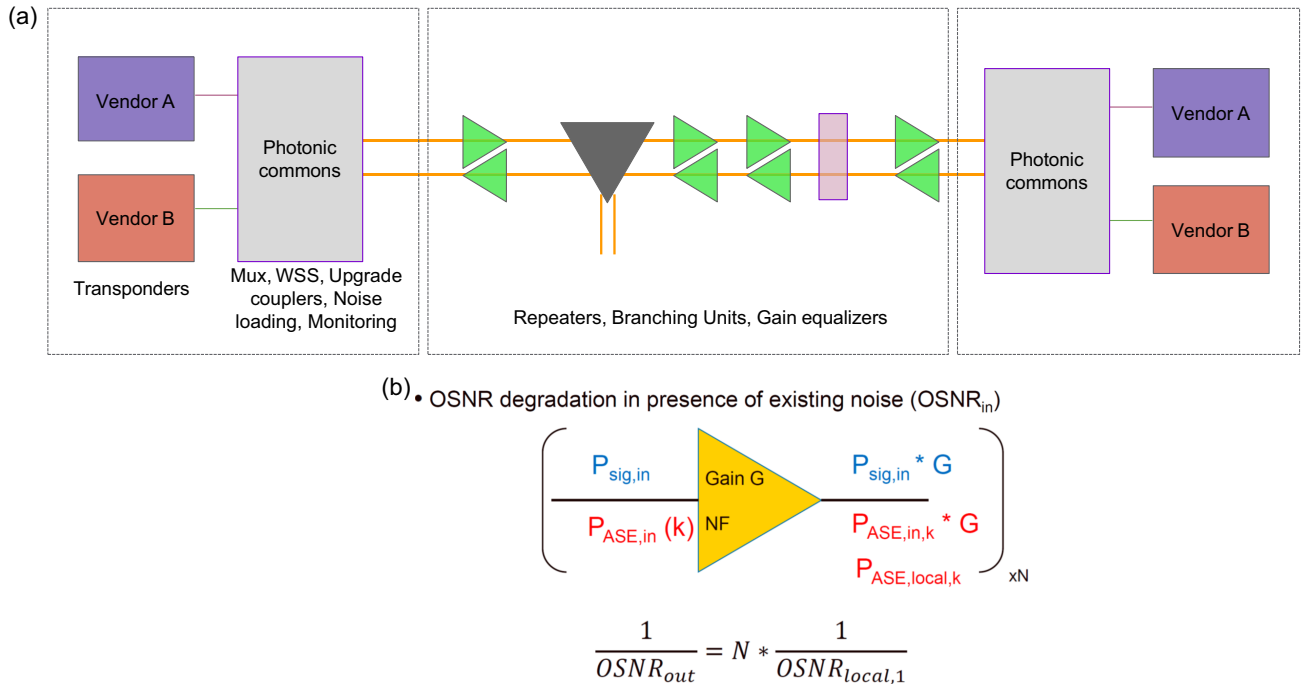

manufacturing variations in fibers produced in large quantities, cabling losses, bend losses, and the effects of deployment in a terrestrial or undersea environment. The assignment of realistic effective loss = ideal loss + 0.01 dB/km for the hollow-core transmission fibers in Table 3 is based on considerations of bend losses, cabling losses, the effects of deployment in demanding subsea/terrestrial environments, and large-scale manufacturing variations with currently installed fiber cables. We expect that this assignment will be refined and made more accurate and precise during the next phases of development as hollow-core fibers optimized for the 2000 nm spectral band are studied more extensively than they have been so far.

With the parameters in Table 3, we now turn to the optical architecture for the future 2000 nm DWDM lightwave transmission system which is shown schematically in Figure 11.

We note that for terrestrial lightwave applications, the east-west distance across Russia is 9,000 km. For subsea lightwave applications, the circumference of the Earth at the equator is 40,075 km. Therefore, we consider 10,000 km and 40,000 km system lengths without O-E-O electronic regeneration and present 2000 nm DWDM lightwave transmission system designs for each of these two significant applications. In our analysis, we follow the OSNR and system margin designs and calculations described and outlined in References [25–30] and Figure 11(b).

We start with the design of a terrestrial lightwave system with total transmission distance of 10,000 km. In this system, we select repeater spans of 200 km corresponding to a span loss and amplifier gain of 10.0 dB and NSPAN = 50. Here we use 350 nm BW fiber amplifiers with 2.2 W total output power and a noise figure of 6.0 dB (in-band pumping as in Figure 2). We choose +33.4 dBm output power from the amplifiers because there are no constraints on the electrical power available for operating the fiber amplifier repeaters for terrestrial lightwave systems.

The general formula for the OSNR (dB, 0.1 nm) for a cascade of NAMP identical fiber amplifier repeaters with gain G = span loss is given by the following expression for 2000 nm lightwave systems [25–30]:

$$\mathrm{OSNR\,(dB/0.1\,nm)} = 60.2 + \mathrm{TOP\,(dBm)} - 10\log10\,(\mathrm{NSPAN}) - \mathrm{G\,(dB)} - \mathrm{NF\,(dB)} - 10\log10\,(\mathrm{NCHAN}) \quad (1)$$

where TOP (dBm) is the total signal power at the output of the fiber amplifier. For the terrestrial system, TOP(dBm) = 33.4, NSPAN = 50, G(dB) = 10.0, NF(dB) = 6.0 (device noise figure), and NCHAN = 571. Using these values in Equation (1) yields, the results in Equation (2):

$$\mathrm{OSNR\ (dB/0.1nm)} = 33.0\,\mathrm{dB\ for\ the\ terrestrial\ system} \quad (2)$$

Since this is in the "large SNR regime" [26], we do not correct this value for generalized droop in concatenated fiber amplified lightwave systems. Following the analysis by He et al. [31], we find that the Q-factor at the receiver for 33.0 dB OSNR/0.1 nm is expected to be 11.0 dB.

We note that this system is completely ASE noise limited since the contribution of all nonlinear effects is zero at this power level [25–30]. Typical terrestrial lightwave systems with this bit rate and modulation format [31] require an OSNR (dB/0.1 nm) ≥24.0 dB and a Q-factor >4.7 dB for successful operation, so this 10,000 km 0.161 Pb/s DWDM system in the 2000 nm band has a high beginning of life (BOL) OSNR margin of +9.0 dB/0.1 nm and Q-factor margin of +6.3 dB, leading to excellent system performance with significant margin to counteract the effects of fiber span aging, variations in amplifier gain with temperature and elapsed time, and other system lifetime considerations. We note that typical OSNR margins in existing simulated ~10,000 km

DWDM lightwave system designs are on the order of 3.0 dB [32], and this observation validates our characterization of 9.0 dB BOL margins as robust for the novel systems presented in this paper.

We next consider design of a submarine lightwave system with total transmission distance of 10,000 km. In this system, we select repeater spans of 100 km corresponding to a span loss and amplifier gain of 5.0 dB and NSPAN = 100. Here we use 350 nm BW fiber amplifiers with 1.00 W total output power and a noise figure of 4.0 dB (out-of-band pumping as in Figure 8). This total output power of +30.0 dBm in each of a pair of fiber amplifiers is constrained by the maximum power available in the subsea cable and is based on an analysis of the fiber amplifier architecture in Figure 8 and the analysis of Meseguer et al. [28], Poggiolini and Poletti [25], as well as Inada [33] for powering of subsea cables using a maximum available electrical power for the cable of 18 kW net and a cable resistance of 1.0 ohms/km. For this subsea amplifier design, the optical-to-optical conversion efficiency is 18%, and the electrical-to-optical conversion efficiency is 3.5%. A detailed analysis of the power budgets will be presented in a future publication.

The relevant parameters for the 10,000 km subsea system operation are now the following: TOP(dBm) = 30.0, NSPAN = 100, G(dB) = 5.0, NF(dB) = 4.0 (device noise figure), and NCHAN = 571. Using these values in Equation (1) yields, the result in Equation (3):

$$\text{OSNR}\ (\text{dB}/0.1\,\text{nm}) = 33.6\,\text{dB for the submarine system} \quad (3)$$

which corresponds to a Q-factor of 11.6 dB [31]. We note that this system is also completely ASE noise limited since the contribution of all nonlinear effects is zero at this power level [27, 28]. Typical lightwave systems with this bit rate and modulation format [31] require an OSNR (dB/0.1 nm) ≥24.0 dB and a Q-factor of 4.7 dB for successful operation, so this 10,000 km 0.161 Pb/s DWDM system in the 2000 nm band has a BOL OSNR margin of +9.6 dB/0.1 nm and Q-factor margin of +6.9 dB, leading again to excellent BOL system performance with significant margin to counteract the effects of system lifetime considerations. The capacity × distance product for this subsea system with robust margins is 1.61 Exabits/s. km.

We observe that the typical OSNR (dB/0.1 nm) margin between best BOL target performance and worst end-of-life (EOL) system performance for open subsea lightwave transmission systems is 4.5 dB as derived from a 2000 nm adaptation of Table 2 in Rivera Hartling et al. [34] and also from ITU-T G-series Recommendations – Supplement 39 [35]. Therefore, the 10,000 km subsea design presented here is expected to operate successfully at both BOL and EOL.

We next consider the maximum distance that can be achieved with the subsea lightwave system design if we keep the above BOL-EOL margin of 4.5 dB constant and use the additional overhead of (9.6 dB – 4.5 dB) = 5.1 dB to increase the transmission distance. We also decrease the number of channels from 571 to 440 yielding an additional increase in OSNR of 1.13 dB and a total transmission capacity of 0.124 Pb/s. The increase in NPAN is now 5.1 dB + 1.13 dB = 6.23 dB or a linear factor of $10^{(0.623)} = 4.198$ to yield an increased number of spans of ~420 and a total transmission distance of 41,980 km. We observe that the circumference of the Earth at the equator is 40,075 km.

Therefore, we predict it is now possible to circumnavigate the Earth with an unrepeatered (no O-E-O electronic functions), all-optical fiber optic DWDM lightwave transmission system having a total capacity of 0.124 Pb/s in one direction and 4.5 dB OSNR BOL margin, and one single core fiber pair. The capacity-distance product for this deployable design is 5.21 Exabits/s. km. Powering of the all-optical subsea cable system may be accomplished by using ≤10,000 km segments between landing points each operated with the powering strategy described above, and ROADM functions for the all-optical lightwave 2000 nm DWDM transmission at each landing point.

This observation leads to a thought experiment: What additional transmission distance can be achieved in a hero research experiment where the OSNR margin is 0.0 dB, and the system is just at the threshold of errors for BER = 1E–03? From the analysis above we see that the total distance and number of spans will be increased from 41,980 km and 420 by a linear factor of $10^{(0.45)} = 2.818$ to NSPAN = 1184 and total transmission distance = 118,300 km. The corresponding capacity-distance product is now 14.67 Exabits/s. km. It will be interesting to conceive of, and then design and implement, a recirculating loop DWDM experiment in the laboratory capable of transmitting over 118,300 km or about 3 times the circumference of the Earth at the equator.

Table 4 below presents a summary outline of the results of the system simulations and outcomes presented so far.

We next discuss an important metric for ultra-high-capacity DWDM lightwave transmission systems: the dependence of Q-factor on the transmitted optical launch power per individual channel. In a conventional high-capacity DWDM lightwave system using existing silica core transmission fibers, a typical Q-factor vs. launch power curve is shown below in Figure 12(a) [36].

We observe that in this typical curve for existing systems, the nonlinear effects in the transmission fiber significantly limit the maximum optical power per channel that can be launched, and the typical dependence is an inverted parabolic curve with a maximum Q-value at quite low powers as shown in Figure 12(a). In contrast, the 10,000 km submarine system design has no nonlinear effects at the power levels considered, and as a result, the predicted Q-factor vs. per-channel launch power curve follows a linear dependence as shown in Figure 12(b).

Following the analysis in Meseguer et al. [28] as well as Poggiolini and Poletti [25] we expect the threshold for the onset of nonlinearities in the DNANF hollow-core transmission fiber in our 10,000 and 40,000 km submarine system designs to be at least three orders of magnitude greater than the launched powers employed in our present calculations.

We finally compare the design performance of our proposed novel 40,000 km 2000 nm Pb/s DWDM subsea lightwave system with historical trends over the past 30 years [37, 38]. This comparison is presented in Figure 13 [37, 38] which contains a timeline of research and deployed product capacity × distance capabilities for unregenerated optical data transmission over a single one-core optical fiber. We see that the proposed novel 2000 nm DWDM subsea lightwave system introduced in this work is projected to outperform the 30-year historical trends by a factor of ~10 or greater. This projected improvement in overall performance validates our novel design approach and points the

Table 4
Summary of capacity × distance products for the 2000 nm DWDM lightwave systems under study

Lightwave system application	Deployable system distance × capacity	Research experiment distance × capacity
10,000 km Terrestrial	1.61 Exabits/s. km	
10,000 km Subsea	1.61 Exabits/s. km	
40,000 km Subsea	5.21 Exabit/s. km	
118,300 km Subsea		14.67 Exabit/s. km

Figure 12
(a) Q versus per-channel launch power for two transmit precompensation values for WaveLogic 3 100 Gb/s DP-QPSK after 5000 km and (b) Q-factor vs. launched optical power per-channel dependence for the 10,000 km submarine lightwave system design. The nominal power per channel for the subsea system is +2.5 dBm

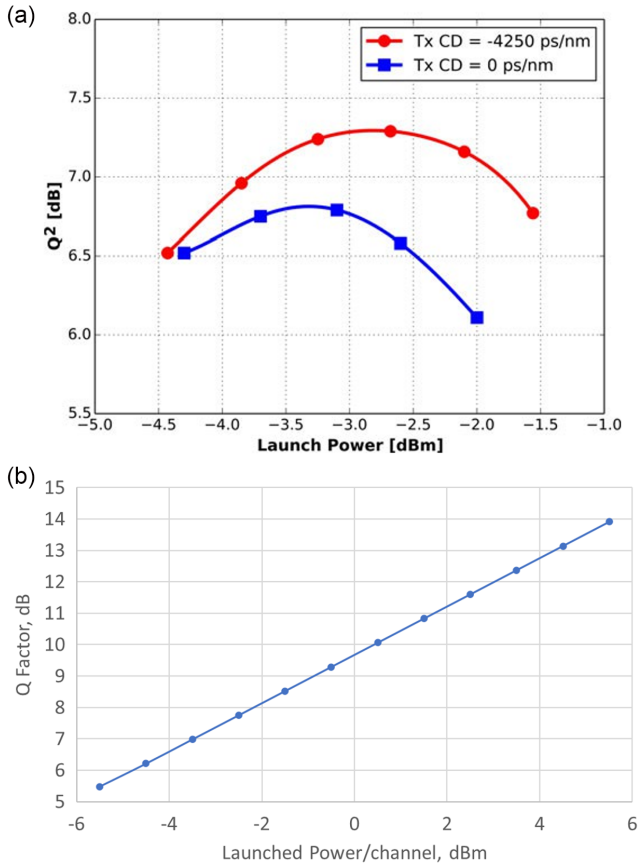

way to new system designs with 10,000 km and 40,000 km unregenerated Pb/s DWDM data transmission capabilities.

4. Discussion and Summary

We first observe that all the novel designs and performances for the fiber amplifiers presented here are the result of simulations and not experiments. Nevertheless, we also observe that the simulators employed in this study have been shown in many publications to have achieved an accuracy of ±0.5 dB in saturated output power and ±1.0 dB in small signal gains for both Tm-doped and Ho-doped fiber lasers and amplifiers when compared with experimental results as outlined in detail in Tench et al. [7], Tench et al. [21] and Romano et al. [19]. Based on these demonstrated results, we are confident that our designs are both precise and accurate and provide a full, fair, and complete representation of the performance of our novel broadband fiber amplifiers in the 2000 nm band.

We next observe that isolators, circulators, WDMs, and gain-flattening filters with an operating bandwidth of ~400 nm at 2000 nm are expected to be available soon based on the recent progress in this field of infrared component development. As an example, typical operating bandwidths for today's optical isolators and circulators in the 2000 nm spectral band are about <1890–>2130 nm or >240 nm. The same is true for the production of new realistically deployable hollow-core fibers with appropriate loss vs. wavelength and dispersion characteristics in the 2000 nm band, such as the loss vs. wavelength plots illustrated in Figure 9 [17]. Great progress has already recently been demonstrated, and greater progress will soon be achieved, in the development of the novel wideband optical components and hollow-core fibers for future 2000 nm DWDM lightwave transmission systems.

We note that the expected chromatic dispersion effects with the novel hollow-core fiber designs [26, 28] over the ≥10,000 km distances considered here can readily be compensated by existing techniques in coherent lightwave transmission systems. The PCS-64QAM modulation technique is employed to provide compensation for any potential nonlinearities experienced in the 100 to 200 concatenated fiber amplifiers in the system designs. Other anticipated transmission effects, such as polarization, PMD, and optical filtering, will depend on the development of DNANF hollow-core fibers and are under study in many venues at the present time. Realistic powering of the submarine cable at ≥10,000 km total length can be achieved by selecting appropriate electrical powering of the cable sections as discussed above and in Meseguer et al. [27], Poggiolini and Poletti [25], and Inada [33].

In summary, we have reported the design and applications of a multi-Watt 2000 nm band hybrid Tm- and Ho-doped fiber amplifier with record wideband 380 nm (31.5 THz) continuously operating bandwidth from 1720 to 2100 nm. We outlined the theory, physics, and simulations behind this design, and showed by comparison with previously published experimental results that the design presented here is accurate to within ±0.5 dB in signal output power and ±1.0 dB in small signal gain.

In our detailed studies of unregenerated 10,000 km terrestrial and submarine lightwave systems, we demonstrated predicted 0.161 Pb/s DWDM system capacities with novel and robust +9.0 dB/0.1 nm and +9.6 dB/0.1 nm OSNR BOL operating margins, respectively. The predicted BOL Q-factor margins for terrestrial and subsea systems are +6.3 dB and +6.9 dB, respectively. (The effects of aging and other impairments leading to realistic EOL margin calculations will be presented in a future publication.) We achieved a total capacity × distance product of 1608 Pb/s. km (1.61 Exabits/s. km) over a single one-core optical fiber for the 10,000 km system designs.

Applications to 40,000 km unregenerated all-optical DWDM 0.124 Pb/s subsea lightwave transmission with deployable BOL OSNR and Q-factor margins and a capacity × distance product of 5.21 Exabits/s. km were also outlined. We note that a 40,000 km all-optical unregenerated subsea/terrestrial system design would provide new connectivity and system architecture possibilities that are impossible today. For example, a subsea/terrestrial all-optical ring system circumnavigating the Earth, which could be named North-South TransGlobal I, can now be designed to provide essential interconnections in the north-south directions that do not exist today. This novel system will greatly enhance the connectivity, redundancy, and reliability of service in the worldwide lightwave transmission network.

Our calculations clearly show that our novel approach yields 2000 nm DWDM system performances that greatly exceed anything possible today or tomorrow with C- and L-band transmission in the 1550 nm region of the spectrum, or O, E, and S-band transmission in the 1300 nm spectral region.

We believe that our proposed 2000 nm Pb/s DWDM subsea and terrestrial lightwave transmission systems with 1608–5420 Pb/s. km (1.61–5.24 Exabits/s. km) capacity × distance product and achievable unregenerated transmission distances of 10,000–40,000 km will be designed, manufactured, deployed, and brought into service within the next five to ten years, and will significantly

Figure 13
Historical and projected trends for unregenerated subsea lightwave transmission through a single one-core optical fiber in terms of capacity-distance product in Exabits/s. km

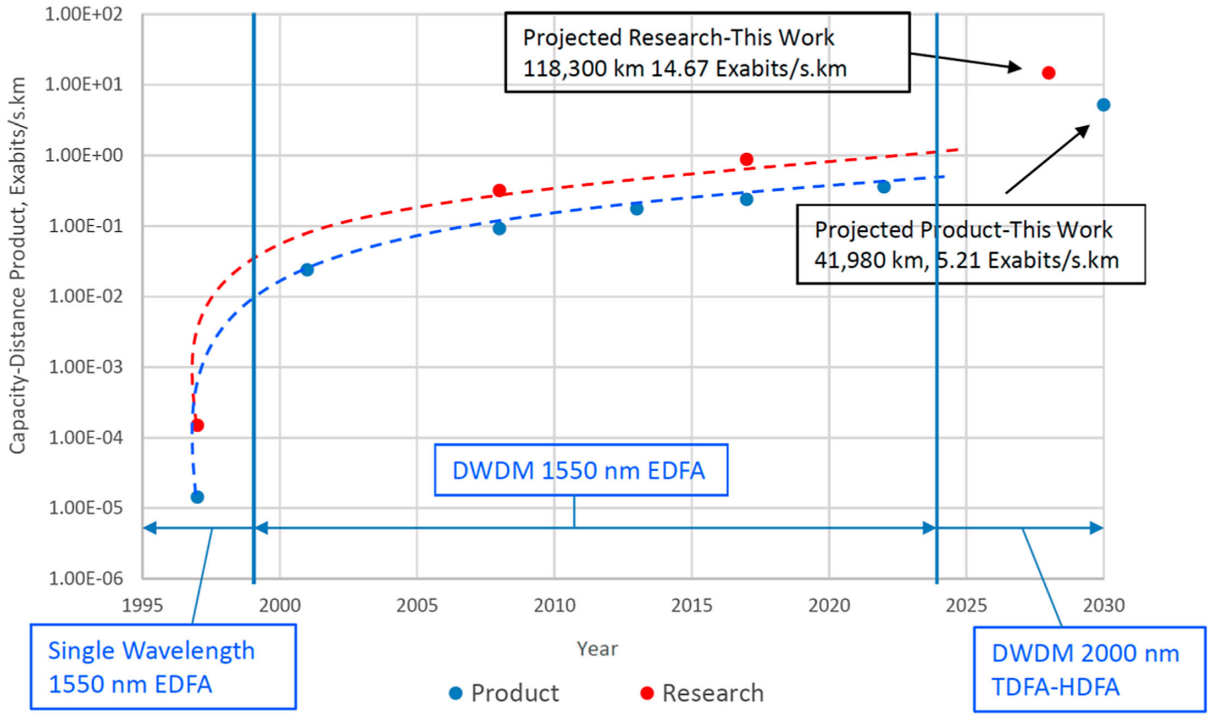

advance the deployment and operation of future terrestrial and subsea DWDM lightwave systems and networks.

5. Methods of Simulation and Calculation

The Ho-doped fiber amplifier simulations are fully described in the techniques section of Reference [21] and are carried out with a proprietary program called Ho-FIB1. The Tm-doped simulations are carried out in a quite similar manner in Romano et al. [19] and are carried out with a proprietary program called Tm-FIB1. The accuracy of the Ho-FIB1 and Tm-FIB1 simulations when compared to experimental results is found to be ±1.0 dB in small signal gain and ±0.5 dB in saturated output power as outlined in detail in Tench et al. [7], Romano et al. [19] and Tench et al. [21].

Funding Support

This work is sponsored by RET and Associates LLC.

Ethical Statement

This study does not contain any studies with human or animal subjects performed by the author.

Conflicts of Interest

The author declares that he has no conflicts of interest to this work.

Data Availability Statement

Exail Tm- and Ho-doped gain fiber specifications are openly available at https://cybel-llc.com/wp-content/uploads/2021/06/IXF-HDF-PM-8-125_edA-Ho-SC-doped-PM-fiber.pdf and https://cybel-llc.com/wp-content/uploads/2021/06/IXF-TDF-PM-5-125_edA-Tm-SC-doped-PM-fiber.pdf. Data of the component devices in Table 1 are openly available at https://retandassociatesllc.com/wp-content/uploads/2024/04/GSLEOP2022-Presentation-RET-v.11-08222022.pdf. Other data are available from the corresponding author upon reasonable request.

Author Contribution Statement

Robert E. Tench: Conceptualization, Methodology, Software, Validation, Formal analysis, Investigation, Resources, Data curation, Writing – original draft, Writing – review & editing, Visualization, Supervision, Project administration, Funding acquisition.

References

[1] Baer, P., Cebeci, P., Reiter, M., Giesberts, M., & Hoffmann, H. D. (2024). 10 W-class, narrow-linewidth, linearly polarized, low-noise holmium-doped fiber amplifier at 2095nm. *Optics Continuum*, *3*(8), 1302–1310. https://doi.org/10.1364/OPTCON.525036

[2] Holmen, L. G., & Fonnum, H. (2021). Holmium-doped fiber amplifier for pumping a $ZnGeP_2$ optical parametric oscillator. *Optics Express*, *29*(6), 8477–8489. https://doi.org/10.1364/OE.419939

[3] Wang, J., Bae, N., Lee, S. B., & Lee, K. (2019). Effects of ion clustering and excited state absorption on the performance of Ho-doped fiber lasers. *Optics Express*, *27*(10), 14283–14297. https://doi.org/10.1364/OE.27.014283

[4] le Gouët, J., Gustave, F., Bourdon, P., Robin, T., Laurent, A., & Cadier, B. (2020). Realization and simulation of high-power holmium doped fiber lasers for long-range transmission. *Optics Express*, *28*(15), 22307–22320. https://doi.org/10.1364/OE.394011

[5] Reiter, M., & Baer, P. (2024). Thermo-optical simulation of holmium-doped fiber amplifiers for high-power applications. *Optics Continuum*, *3*(8), 1516–1527. https://doi.org/10.1364/OPTCON.532149

[6] Filatova, S. A., Fale, A. E., Kamynin, V. A., Wolf, A. A., Zhluktova, I. V., Nanii, O. E., . . . , & Tsvetkov, V. B. (2023). Investigation of absorption dynamics from the excited state $^5I_7$ of holmium ions in optical silica-based fibers. *Journal of Lightwave Technology*, *41*(19), 6400–6407. https://doi.org/10.1109/JLT.2023.3278534

[7] Tench, R. E., Zepeda, A., Walasik, W., Amavigan, A., & Delavaux, J. M. (2024). Design and performance of 1762 nm Tm-doped fiber amplifiers for manipulation and control of optical qubits in ^{133}Ba+ ions. In *Quantum Computing, Communication, and Simulation IV: Proceedings of SPIE*, *12911*, 1291111. https://doi.org/10.1117/12.3001098

[8] Baer, P., Cebeci, P., Reiter, M., Bontke, F., Giesberts, M., & Hoffmann, H. D. (2024). Ultra-low-noise, single-frequency, all-PM Thulium- and Holmium-doped fiber amplifiers at 1950 nm and 2090 nm for third-generation gravitational wave detectors. *IEEE Photonics Journal*, *16*(1), 1–9. https://doi.org/10.1109/JPHOT.2024.3354454

[9] Li, Z., Heidt, A. M., Daniel, J. M. O., Jung, Y., Alam, S. U., & Richardson, D. J. (2013). Thulium-doped fiber amplifier for optical communications at 2 μm. *Optics Express*, *21*(8), 9289–9297. https://doi.org/10.1364/OE.21.009289

[10] Sincore, A., Bradford, J. D., Cook, J., Shah, L., & Richardson, M. C. (2018). High average power thulium-doped silica fiber lasers: Review of systems and concepts. *IEEE Journal of Selected Topics in Quantum Electronics*, *24*(3), 1–8. https://doi.org/10.1109/JSTQE.2017.2775964

[11] Aubrecht, J., Pokorný, J., Švejkarová, B., Kamrádek, M., & Peterka, P. (2024). Broadband thulium fiber amplifier for spectral region located beyond the L-band. *Optics Express*, *32*(10), 17932–17941. https://doi.org/10.1364/OE.522088

[12] Romano, C., Lorenz, D., Eichhorn, M., & Kieleck, C. (2021). Watt-level thulium: Holmium-codoped versus holmium-doped polarization-maintaining fiber amplifier at 2050 and 2090 nm. In *Laser Technology for Defense and Security XVI: Proceedings of SPIE*, *11724*, 117240I. https://doi.org/10.1117/12.2587919

[13] Kadwani, P., Sims, R. A., Chia, J., Altal, F., Shah, L., & Richardson, M. C. (2011). Atmospheric gas detection using broadband mid-IR thulium fiber-based sources. In *Laser Technology for Defense and Security VII: Proceedings of SPIE*, *8039*, 80390L. https://doi.org/10.1117/12.887020

[14] Anderson, B. M., Solomon, J., & Flores, A. (2021). 1.1 kW, beam-combinable thulium doped all-fiber amplifier. In *Fiber Lasers XVIII: Technology and Systems: Proceedings of SPIE*, *11665*, 116650B. https://doi.org/10.1117/12.2576209

[15] Anderson, B., Flores, A., Grosek, J., & Dajani, I. (2017). High power Tm-doped all-fiber amplifier at 2130 nm. In *Conference on Lasers and Electro-Optics*, SM1L.3. https://doi.org/10.1364/CLEO_SI.2017.SM1L.3

[16] Garcia Gunning, F. C., Kavanagh, N., Russell, E., Sheehan, R., O'Callaghan, J., & Corbett, B. (2018). Key enabling technologies for optical communications at 2000 nm. *Applied Optics*, *57*(22), E64–E70. https://doi.org/10.1364/AO.57.000E64

[17] Chen, Y., Petrovich, M. N., Fokoua, E. N., Adamu, A. I., Hassan, M. R. A., Sakr, H., . . . , & Poletti, F. (2024). Hollow core DNANF optical fiber with <0.11 dB/km loss. In *Optical Fiber Communication Conference*, Th4A.8. https://doi.org/10.1364/OFC.2024.Th4A.8

[18] Fokoua, E. N., Abokhamis Mousavi, S., Jasion, G. T., Richardson, D. J., & Poletti, F. (2023). Loss in hollow-core optical fibers: Mechanisms, scaling rules, and limits. *Advances in Optics and Photonics*, *15*(1), 1–85. https://doi.org/10.1364/AOP.470592

[19] Romano, C., Tench, R. E., & Delavaux, J. M. (2018). Simulation of 2μm single clad thulium-doped silica fiber amplifiers by characterization of the $^3F_4$ – $^3H_6$ transition. *Optics Express*, *26*(20), 26080–26092. https://doi.org/10.1364/OE.26.026080

[20] Alyshev, S., Khegai, A., Umnikov, A., & Firstov, S. (2024). Bismuth-doped fiber lasers and amplifiers operating from O- to U-band: Current state of the art and outlook. *Photonics*, *11*(7), 663. https://doi.org/10.3390/photonics11070663

[21] Tench, R. E., Delavaux, J. M., Walasik, W., Amavigan, A., & Jaouen, Y. (2024). 2 μm Watt-level fiber amplifiers, lasers, and ASE sources pumped by broadband ASE pumps. *Journal of Lightwave Technology*, *42*(24), 8881–8888. https://doi.org/10.1109/JLT.2024.3445173

[22] Srivastava, A. K., & Sun, Y. (2002). Advances in erbium-doped fiber amplifiers. In I. P. Kaminow, & T. Li (Eds.), *Optical fiber telecommunications IV-A* (4th ed., pp. 174–212). Academic Press. https://doi.org/10.1016/B978-012395172-4/50004-8

[23] Jackson, S. D., Bugge, F., & Erbert, G. (2007). High-power and highly efficient Tm^{3+} -doped silica fiber lasers pumped with diode lasers operating at 1150 nm. *Optics Letters*, *32*(19), 2873–2875. https://doi.org/10.1364/OL.32.002873

[24] Jackson, S. D., Bugge, F., & Erbert, G. (2007). High-power and highly efficient diode-cladding-pumped Ho^{3+} -doped silica fiber lasers. *Optics Letters*, *32*(22), 3349–3351. https://doi.org/10.1364/OL.32.003349

[25] Poggiolini, P., & Poletti, F. (2022). Opportunities and challenges for long-distance transmission in hollow-core fibres. *Journal of Lightwave Technology*, *40*(6), 1605–1616. https://doi.org/10.1109/JLT.2021.3140114

[26] Bononi, A., Antona, J. C., Serena, P., Carbo-Meseguer, A., & Lasagni, C. (2021). The generalized droop model for submarine fiber-optic systems. *Journal of Lightwave Technology*, *39*(16), 5248–5257. https://doi.org/10.1109/JLT.2021.3080240

[27] Pecci, P., Letellier, V., Gautheron, O., Shelton, A., Courtois, O., Gumier, M., . . . , & Gabla, P. (2018). Design of submarine "open" cables. In *Optical Fiber Communication Conference*, M1D.4. https://doi.org/10.1364/OFC.2018.M1D.4

[28] Meseguer, A. C., Antona, J. C., Esparza, J. U., Calsat, A., Plantady, P., Quintana, A., & Letellier, V. (2022). Experimental assessment of capacity prediction from G-SNR measurements for submarine systems. In *Optical Fiber Communication Conference*, W4G.3. https://doi.org/10.1364/OFC.2022.W4G.3

[29] Meseguer, A. C., de Araujo, J. T., & Antona, J. C. (2023). Multi-core vs hollow-core fibers: Technical study of their viability in SDM power-constrained submarine systems. *Journal of Lightwave Technology*, *41*(12), 4002–4009. https://doi.org/10.1109/JLT.2023.3278714

[30] Meseguer, A. C., Bissessur, H., & Antona, J. C. (2024). Potential of hollow-core fibers for submarine systems. *Optical Fiber Technology*, *84*, 103750. https://doi.org/10.1016/j.yofte.2024.103750

[31] He, X., Jiang, L., Sun, J., Yi, A., Fu, C., Hu, Q., . . . , & Yan, L. (2024). Total net-rate of 27.88 Tb/s full C-band transmission over 4,550 km using 150 km span length and high-gain EDFA amplification. *Optics Express*, *32*(8), 13500–13507. https://doi.org/10.1364/OE.517730

[32] Downie, J. D. (2018). Maximum capacities in submarine cables with fixed power constraints for C-band, C+L-band, and multicore fiber systems. *Journal of Lightwave Technology*, *36*(18), 4025–4032. https://doi.org/10.1109/JLT.2018.2858194

[33] Inada, Y. (2022). *Cable powering* [Lecture notes]. https://www.optica.org/events/meeting_archives/2022/subsea_optical_fiber_communications/#Speakers

[34] Rivera Hartling, E., Pilipetskii, A., Evans, D., Mateo, E., Salsi, M., Pecci, P., & Mehta, P. (2021). Design, acceptance and capacity of subsea open cables. *Journal of Lightwave Technology*, *39*(3), 742–756. https://doi.org/10.1109/JLT.2020.3045389

[35] International Telecommunication Union. (2016). *Optical system design and engineering considerations*. Retrieved from: https://www.itu.int/rec/dologin_pub.asp?lang=e&id=T-REC-G.Sup39-201602-I!!PDF-E&type=items

[36] Roberts, K., Foo, S. H., Moyer, M., Hubbard, M., Sinclair, A., Gaudette, J., & Laperle, C. (2015). High capacity transport—100G and beyond. *Journal of Lightwave Technology*, *33*(3), 563–578. https://doi.org/10.1109/JLT.2014.2358203

[37] Winzer, P. J., Neilson, D. T., & Chraplyvy, A. R. (2018). Fiber-optic transmission and networking: The previous 20 and the next 20 years. *Optics Express*, *26*(18), 24190–24239. https://doi.org/10.1364/OE.26.024190

[38] Papapavlou, C., Paximadis, K., Uzunidis, D., & Tomkos, I. (2022). Toward SDM-based submarine optical networks: A review of their evolution and upcoming trends. *Telecom*, *3*(2), 234–280. https://doi.org/10.3390/telecom3020015

How to Cite: Tench, R. E. (2025). Design of a Novel 31.5 THz Bandwidth Hybrid TDFA-HDFA at 2000 nm and Its Applications in Unregenerated DWDM Lightwave Transmission Systems. *Journal of Optics and Photonics Research*. https://doi.org/10.47852/bonviewJOPR42024305